Chinese Chemical Letters 35 (2024) 109386

Contents lists available at ScienceDirect

Chinese Chemical Letters

journal homepage: www.elsevier.com/locate/cclet

Galvanostatic method assembled ZIFs nanostructure as novel nanozyme for the glucose oxidation and biosensing

Erzhuo Cheng[a,1], Yunyi Li[b,1], Wei Yuan[a], Wei Gong[c], Yanjun Cai[a], Yuan Gu[a], Yong Jiang[a], Yu Chen[a], Jingxi Zhang[a], Guangquan Mo[a,*], Bin Yang[a,*]

[a] The Fourth Affiliated Hospital of Guangzhou Medical University, School of Biomedical Engineering, Guangzhou Medical University, Guangzhou 511436, China
[b] Department of Nephrology, First Affiliated Hospital of Jinan University, Guangzhou 510630, China
[c] Department of Oncology, Xiangyang Central Hospital of Hubei University of Arts and Science, Xiangyang 441000, China

ARTICLE INFO

Article history:
Received 9 October 2023
Revised 6 December 2023
Accepted 7 December 2023
Available online 11 December 2023

Keywords:
Sensor
MOFs
Electrocatalytic oxidation
Electrochemical assembly
Glucose

ABSTRACT

Recently, the composite of soft conductive substrates, such as carbon fiber (CF), with metal-organic frameworks (MOFs) has been employed in a myriad of applications. The composite material has demonstrated exceptional potential in the realm of electrochemical sensing platforms. However, the rapid growth of MOFs on the surface of CF remains a challenge. Herein, we propose a simple galvanostatic method as an effective strategy for rapidly growing zeolitic imidazolate frameworks (ZIFs) on CF, and obtain nanocaltrop-like ZIFs modified CF (NC-ZIFs/CF) glucose (Glu) sensor platform with distinctive morphology. The prepared NC-ZIFs/CF demonstrated significant electrocatalytic activity towards the oxidation of Glu in alkaline media, characterized by a pronounced augmentation in oxidation current density. At an applied potential of 0.4 V, NC-ZIFs/CF exhibited a remarkably broad detection range (3–30,000 μmol/L) and demonstrated outstanding selectivity, repeatability and reproducibility. Additionally, the NC-ZIFs/CF was efficaciously employed for the detection of blood Glu levels in the serum of both normoglycemic and hyperglycemic patients, obtaining highly reliable results. This work demonstrates the feasibility of using galvanostatic method assembly to induce the growth of MOFs on conductive substrates, providing new ideas for electrocatalysis sensors and other electrochemical applications.

In the past two decades, metal-organic frameworks (MOFs) have gained considerable attention globally in multiple research fields as a significant new class of materials [1,2]. MOFs are crystalline porous materials that consist of metal cations (nodes) and organic ligands with multiple binding sites (linkers), forming a net-like structure through strong bonds [3]. Due to the nearly infinite combinations of metals and ligands, thousands of novel MOFs variants have been synthesized annually. At the same time, explosive progress in research and applications related to MOFs has been performed [4]. Compared to traditional materials, MOFs offer advantages such as adjustable pore size, high specific surface area, diverse topologies, and the ability to functionalize the pore surfaces [5]. Therefore, MOFs possess the unique capability to be tailored to specific application requirements in diverse scenarios, rendering them highly advantageous and promising for a wide range of applications, including gas storage and separation, supercapacitors, electrochemical sensing, water oxidation, drug delivery, heterogeneous catalysis, and environmental purification [6–10]. Despite the wide variety of MOFs, zeolitic imidazolate frameworks (ZIFs) stand out as one of the subclasses of MOFs due to their extraordinary thermal stability and chemical stability. ZIFs are synthesized through metal-organic coordination reactions between transition metal ions (such as Zn^{2+} and Co^{2+}) as nodes and imidazolates as linkers [11,12]. Since the emergence of ZIFs, they have attracted great interest in various research fields, attributed to their available materials, mild preparation procedures, and excellent properties [13].

However, it is worth noting that ZIFs typically exist in powder form and exhibit low conductivity or even non-conductivity, which limits their suitability as electrode materials for electrochemical applications [5]. Nevertheless, this limitation does not hinder the application potential of MOFs as new materials. Recently, composites composed of MOFs and conductive materials have provided new ideas for designing electrochemical platforms and have shown promising progress [14–18]. Carbon fiber (CF), a highly conductive material, exhibits excellent mechanical flexibil-

* Corresponding authors.
E-mail addresses: gqmo@gzhmu.edu.cn (G. Mo), bin.yang@gzhmu.edu.cn (B. Yang).
[1] These authors contributed equally to this work.

https://doi.org/10.1016/j.cclet.2023.109386
1001-8417/

ity and strength, making it an ideal conductive substrate widely used in various electrochemistry fields [19]. In recent years, many scholars have prepared composite materials containing MOFs and CF for various fields [20]. For instance, Liu and collaborators utilized a vapor-phase method to grow well-arranged Co-MOFs on CF using metal hydroxyfluorides with different morphologies as self-sacrificing templates [18]. Furthermore, by employing typical solution-based or solvent-thermal methods, MOFs nanostructures can be grown on CF to obtain MOFs-composite electrodes with excellent performance for batteries, supercapacitors and electrocatalysis. Chen *et al*. also successfully deposited MOF-525 on CF using conductive adhesive and utilized it as an electrocatalyst for the counter electrode of dye-sensitized solar cells [6]. Interestingly, MOFs can even be grown directly on electrodes without any further treatment. Wei *et al*. developed a non-enzymatic sensing platform for the electrocatalysis of Glu by growing Co-MOFs on CF *via* environmental liquid deposition [15]. In the study of Glu electrochemical sensing research, the utilization of natural enzymes is often impeded by their high cost, lack of long-term stability, and the intricate nature of the fixation process [21,22]. Consequently, the pursuit of alternative solutions has become a necessity. Precious metal nanoenzymes, such as gold and platinum, exhibit commendable electrocatalytic activity [23]. However, their prohibitive cost poses a significant barrier to their large-scale application. Therefore, cobalt-based materials, along with their hydroxides, oxides, and complexes, are an ideal class of nanoenzymes. This is due to their excellent electrocatalytic activity towards Glu and the easy accessibility of raw materials [24,25]. Among them, Co-MOFs, as a typical representative of cobalt-based materials, are widely used in Glu detection due to their large specific surface area and abundant active sites. These advantages may confer upon Co-ZIFs excellent electrocatalytic activity against Glu [26–28]. However, despite the tremendous potential of composite electrodes supported by MOFs nanostructures for practical applications in electrochemical sensors, their utility is constrained by the limited methodologies available for their preparation, detection and electrocatalytic targets. Therefore, it is of heuristic interest to develop a new method for constructing these composites.

In Scheme 1, the classical process of electrochemical assembly of nano-caltrop-like ZIFs on CF is depicted. Since metal ions will move from bulk solution to the surface of CF by electrostatic force. Therefore, in this work, the galvanostatic method was employed to apply a cathode current to the working electrode. This facilitated the adsorption of positively charged Co^{2+} nodes, a strong coordinate bond is formed with the 2-methylimidazole (2-mIM) linkers, resulting in the formation of nano-caltrop-like ZIFs modified CF (NC-ZIFs/CF). Please refer to the Supporting information for detailed experimental procedures. Besides, the incorporation of highly conductive substrates, such as nickel foam, could serve to enhance materials that exhibit poor conductivity. According to the experimental results, dense and uniform NC-ZIFs/CF can be formed under the conditions of 30 μA and 40 min (Fig. 1, Fig. S2 in Supporting information). Fig. 1 provides a visual representation of the scanning electron microscopy (SEM) analysis conducted on NF-ZIFs/CF. In contrast to the immaculate and smooth surface observed on the original bare CF, the adoption of the electrochemical assembly strategy, employing the constant current method, expeditiously enables comprehensive coverage of the CF surface with a layer of nanostructured ZIFs (Fig. S1 in Supporting information). This new method offers gentler and easier experimental steps compared to existing methods, which typically require longer reaction times and more complex reaction conditions. Notably, a completely new morphology emerges for ZIFs grown on the CF surface using the galvanostatic method. Specifically, caltrop-like nanostructured ZIFs uniformly and densely cover the smooth CF surface. Furthermore, compared with the previously reported MOFs grown on conductive substrates, the NC-ZIFs/CF is not only decorated with irregular protrusions but also have a fuller thickness, which may facilitate the exposure of more metal active sites (Fig. S3 in Supporting information) [29–31]. Consequently, this property may confer the excellent electrochemical properties of NC-ZIFs/CF. According to the energy spectrum data (ESD), the CF surface has a coating of nano structure, mainly containing C, N, and Co elements. To substantiate the existence of ZIFs exhibiting a nanoscale caltrop structure, we employed locally-developed nano-caltrop-like ZIFs for transmission electron microscopy (TEM) to comprehensively analyze their structural characteristics. Fig. 2a illustrates a nano-caltrop-like structure, with dimensions approximately 300 nm × 700 nm. Within this structure, the framework of the nano-caltrop-like ZIFs are distinctly visible. Fig. 2b showcases the high-angle annular dark-field scanning transmission electron microscopy (HAADF-STEM) image of nano-caltrop-like ZIFs. This image provides an accurate depiction of the shape and size of the nano-caltrop-like ZIFs, thereby revealing the unique nano-caltrop-like morphology. The observed nano-caltrop-like structure underwent local energy dispersive spectrometer (EDS) mapping. Nano-caltrop-like ZIFs predominantly comprise C, N, and Co elements (Figs. 2c–e), wherein Co is derived from the Co^{2+} node and N from the 2-mIM linker. The X-ray photoelectron spectroscopy (XPS) results further validate the mapping findings. As depicted in

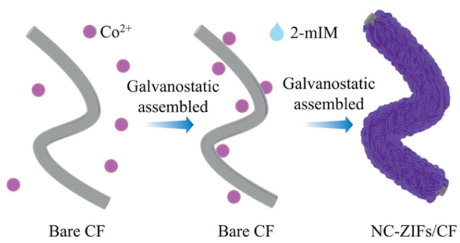

Scheme 1. Scheme presentation of electrochemical assembly of nano-caltrop-like ZIFs on CF.

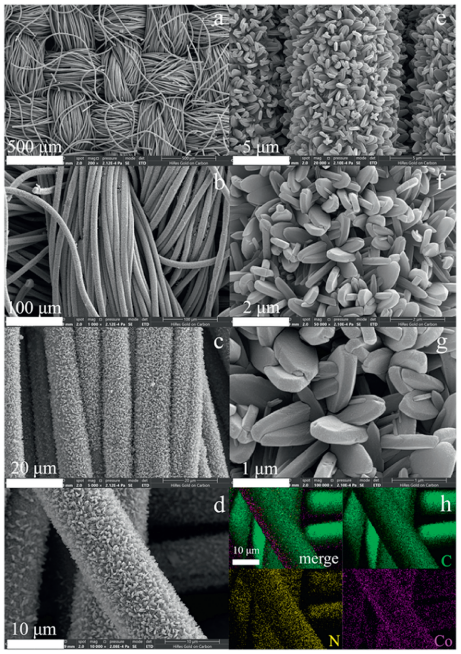

Fig. 1. (a–g) SEM image of nano-caltrop structure covered on NC-ZIFs/CF surface after 40 min growth at 30 μA. (h) EDS mapping of NC-ZIFs/CF. EDS images clearly demonstrated the presence of Co and N elements, indicating that ZIFs had successfully grown on the surface of CF.

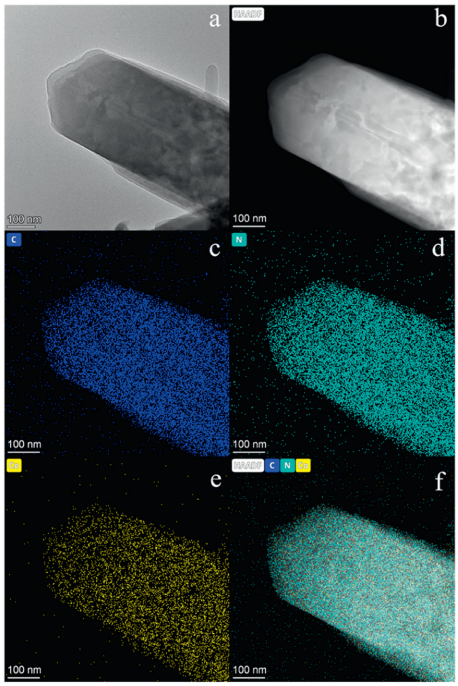

Fig. 2. (a) Local cross section TEM image of NC-ZIFs/CF. (b) HAADF-STEM image of NC-ZIFs/CF. (c–f) HAADF EDS mappings of NC-ZIFs/CF.

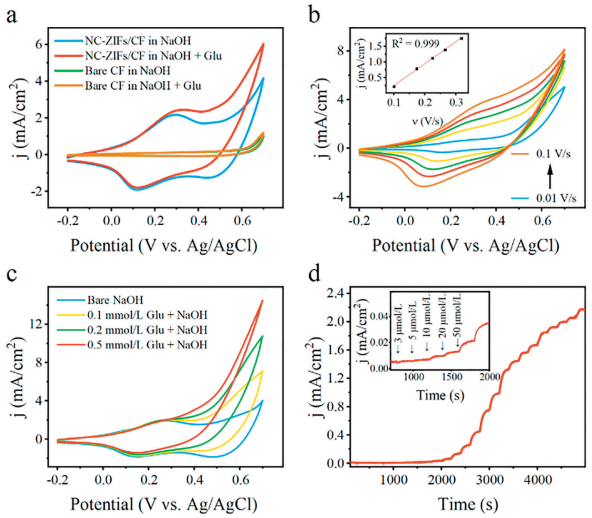

Fig. 3. (a) CV curve of bare CF (green lines) and NC-ZIFs/CF (blue lines) in 0.1 mol/L NaOH. CV curve of bare CF (orange lines) and NC-ZIFs/CF (red lines) in 0.1 mol/L NaOH containing 0.2 mmol/L Glu, scan rate: 0.05 V/s. (b) CV curve of NC-ZIFs/CF at different scan rate (0.01, 0.03, 0.05, 0.07, 0.1 V/s) in 0.1 mol/L NaOH with 0.2 mmol/L Glu, inset is the linear regression analysis between peak current density and scan rate. (c) CV curves of NC-ZIFs/CF at different Glu concentrations in 0.1 mol/L NaOH solution. (d) The *i-t* curve of NC-ZIFs/CF in 0.1 mol/L NaOH with working potential at 0.4 V, scan rate: 0.05 V/s.

Fig. S4a (in Supporting information), nano-caltrop-like ZIFs exhibit characteristic peaks of C 1s, N 1s, and Co 2p, thus corroborating the mapping results. Additionally, X-ray diffraction (XRD) analysis reveals that NF-ZIFs/CF demonstrates several subtle diffraction peaks within the angular range of 5°–30°. This is in contrast to the untreated naked CF, and bears a striking resemblance to the XRD pattern of leaf-like ZIFs (ZIFs-L). To further substantiate this observation, the precipitates obtained after NC-ZIFs/CF preparation were collected and subjected to XRD analysis, yielding results akin to ZIFs-L. These results indicate that NC-ZIFs/CF shares the same crystal type as ZIFs-L (Fig. S4b in Supporting information) [32]. The formation of the nano-caltrop-like structure during the electrochemical assembly may be responsible for the observed changes in diffraction intensity at specific 2θ angles.

In previous reports, ZIF-67 has been used for the quantitative detection of Glu in alkaline solution. Before the formal test, NC-ZIFs/CF was tested 30 times by cyclic voltammetry (CV) at 0.1 mol/L NaOH solution to stabilize the electrochemical performance of NC-ZIFs/CF. To probe the electrocatalytic response of NC-ZIFs/CF towards Glu, the scanning speed was set to 50 mV/s, and CV was employed to investigate the electrochemical characteristics of bare CF and NC-ZIFs/CF in different solutions. As depicted in Fig. 3a, the bare CF did not exhibit any reduction-oxidation peaks in the presence of only 0.1 mol/L NaOH (green line). In contrast, a pair of reduction-oxidation peaks is distinctly observable for NC-ZIFs/CF (blue line). When upon the addition of 0.2 mmol/L Glu, the change in the oxidation current density of bare CF was almost negligible compared to the oxidation current density in the presence of only 0.1 mol/L NaOH (orange line). However, it was observed That the anodic peak current of NC-ZIFs/CF experienced a significant increase following the addition of 0.2 mmol/L Glu. This is evidenced by the enhanced oxidation current density (red line). More specifically, according to previously reported studies, cobalt ions (Co^{2+}) can be oxidized to CoOOH (Co^{3+}) in an alkaline solution, followed by further oxidation of CoOOH (Co^{3+}) to Co^{4+}. It therefore exhibits an anodic peak at about 0.26 V. Glu is oxidized by Co^{4+} under alkaline conditions, and Co^{4+} is reduced to Co^{3+}. It can be observed that the reduction current (red line) at around 0.42 V is much lower than without Glu (blue line), which may be attributed to the consumption of Co^{4+} by Glu [33]. Finally, Co^{3+} is reduced to Co^{2+} at around 0.1 V. This series of reactions is manifested by the formation of two pairs of redox peaks at approximately 0.42 V and 0.1 V, respectively [34,35]. Therefore, we infer that the electrocatalytic mechanism of Glu may be based on the following Eqs. 1–3:

$$Co^{2+} + n\ OH^- + H_2O \leftrightarrow CoOOH + n\ e^- \quad (1)$$

$$CoOOH + H_2O \leftrightarrow Co^{4+} + 3OH^- + e^- \quad (2)$$

$$Co^{4+} + Glu \rightarrow CoOOH + glucolactone + H_2O \quad (3)$$

After the CV test, SEM analysis of the catalyzed NC-ZIFs/CF was performed. As shown in Fig. S5 (in Supporting information), disordered nanocrystalline faces appear, which may be due to the weak coordination between Co^{2+} and organic linkers under the condition of electrocatalysis in alkaline conditions. The released Co^{2+} reacts with OH^- and is further oxidized to CoOOH. Moreover, a slight positive shift of the anode peak and a slight negative shift of the cathode peak were observed as the scan rate increased. Within the range of 0.01–0.1 V/s, the oxidation current density increased linearly with the square root of the scanning rate, with the linear regression coefficient being 0.999 (inset in Fig. 3b). This finding suggests that the oxidation of Glu by the NC-ZIFs/CF surface follows a diffusion-controlled electrochemical process [36]. It is noteworthy that the anodic peak current for Glu oxidation exhibits a proportional increase with the rise in Glu concentration (0.1–0.5 mmol/L), demonstrating a robust linear relationship (Fig. 3c). These findings suggest the feasibility of establishing a voltametric assay for the quantitative determination of Glu without enzyme.

Upon the affirmation of the electrocatalytic activity of NC-ZIFs/CF towards Glu, the amperometric *i-t* curve (*i-t*) methodology was employed to precisely quantify the redox current response

of NC-ZIFs/CF to Glu. In Fig. S6a (Supporting information), we illustrate the effect of different potentials on the voltametric response of Glu when 5 mmol/L Glu is added dropwise into a 0.1 mol/L NaOH solution at 200-second intervals. The results clearly indicate that NC-ZIFs/CF exhibits a significant response to Glu at 0.4 V. Consequently, an applied potential of 0.4 V is selected for NC-ZIFs/CF. This applied potential not only ensures a high current response but also avoids other reactions that may occur at a higher applied potential, such as the influence of interfering substances in the serum, thus improving the anti-interference ability of the sensor. In order to investigate the relationship between current density and Glu concentration, we added different concentrations of Glu into a 0.1 mol/L sodium hydroxide solution at 200-second intervals, and recorded the corresponding current. As depicted in Fig. 3d, the response current density showed a progressive increase with a gradual rise in Glu concentration. The inset of Fig. 3d further confirms the lowest response concentration of Glu to be 3 μmol/L. Furthermore, we delineated three distinct linear ranges: 3 μmol/L–1 mmol/L with a current sensitivity of 0.2553 mA cm^{-2} $mmol^{-1}$, 1–7.6 mmol/L with a current sensitivity of 0.1528 mA cm^{-2} $mmol^{-1}$, and finally, 7.6–30 mmol/L with a current sensitivity of 0.0429 mA cm^{-2} $mmol^{-1}$. The regression equations correlating Glu concentration (C, mmol/L) and response current density (j, mA/cm^2) were established as follows: $j = 0.2553C + 0.0178$ ($R^2 = 0.998$), $j = 0.1528C + 0.1158$ ($R^2 = 0.990$), and $j = 0.0429C + 0.9543$ ($R^2 = 0.991$), respectively (Fig. S6b in Supporting information). Considering the normal human serum blood Glu concentration ranges from 3 mmol/L to 6 mmol/L, the high linear range of 30 mmol/L is well-suited to meet the monitoring requirements of most people with normoglycemia and hyperglycemia [37]. Therefore, the performance of NC-ZIFs/CF can fulfill most of the measurement requirements. Comparative analysis with previous electrochemical platforms indicated that the performance of NC-ZIFs/CF was significantly better than previous results in one or more respects (Table S1 in Supporting information) and demonstrated reliable accuracy across different glucose concentrations (Table S2 in Supporting information). Besides, selectivity is a critical parameter in evaluating the performance of non-enzyme Glu sensors. Human blood is a highly complex fluid, comprising various ions and biomolecules in abundance. Additionally, the composition of human serum is complex. Glu, as the main energy source of the human body, is extremely abundant in serum. Furthermore, the concentrations of saline ions (Na^+, K^+) closely approximate that of Glu. In human serum, the concentration of other interference is much smaller than that of Glu (less than 1:30) [15,38,39]. Therefore, we used a ratio of 1:30 (physiological level) for interferon to Glu concentration and a 1:20 ratio (higher than physiological level) for selective testing [40,41]. Consequently, to assess the interference resistance of NC-ZIFs/CF, we selected representative interfering substances, namely NaCl, KCl, uric acid (UA), citric acid (CA), ascorbic acid (AA), and dopamine (DA). In determining the concentrations of interfering substances, we matched the concentrations of various ions with that of added Glu based on actual blood conditions. As demonstrated in Fig. 4a, an initial addition of 0.5 mmol/L Glu was followed by 0.5 mmol/L NaCl and KCl, as well as 16.7 μmol/L of DA, UA, AA, and CA. Subsequently, the Glu concentration was adjusted to 1 mmol/L, and accordingly, the concentrations of NaCl and KCl were also adjusted to 1 mmol/L, while the other interfering substances were adjusted to one-twentieth of the Glu concentration, specifically 50 μmol/L. As depicted in the Figs. 4a and b, the changes in current response induced by these interfering substances were negligible, underscoring the robust resistance of NC-ZIFs/CF to interfering substances under physiological conditions. Consequently, the NC-ZIFs/CF sensor exhibits a remarkable capacity for highly selective Glu detection. In order to assess the repeatability, reproducibility, and long-term stability of the NC-

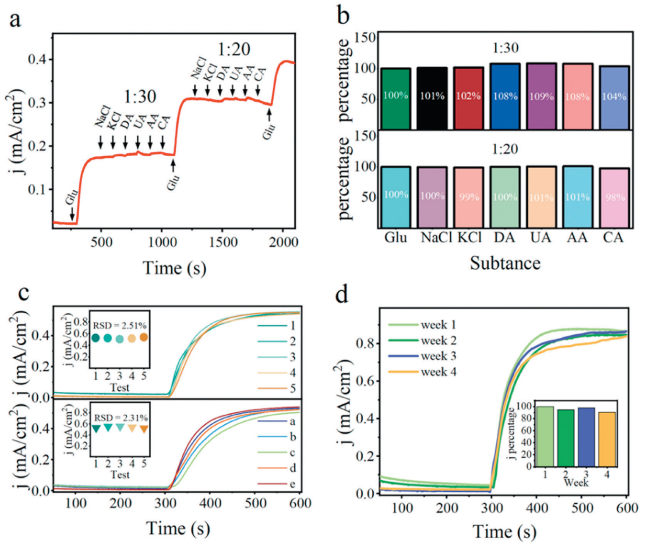

Fig. 4. (a) The *i-t* curve of the NC-ZIFs/CF toward the successive addition of different concentrations of Glu, NaCl, KCl, DA, UA, AA, CA, in a stirred 0.1 mol/L NaOH. (b) The peak current density percentage of Glu in solution with interfering substances. (c) The *i-t* curves in 0.1 mol/L NaOH with 3 mmol/L Glu for five tests at one NC-ZIFs/CF sensor, inset is the peak current density of each test (top image). The *i-t* curves in 0.1 mol/L NaOH with 3 mmol/L Glu for five newly prepared sensors, inset is the peak current density of each sensor (bottom image). (d) The *i-t* curve in 0.1 mol/L NaOH with 5 mmol/L Glu from the first week to fourth week. Inset is the peak current density percentage of each detection.

ZIFs/CF sensor, a two-step evaluation was conducted. Firstly, the identical sensor was subjected to five consecutive measurements of a Glu solution, resulting in a relative standard deviation (RSD) of 2.31%. Secondly, five newly prepared NC-ZIFs/CF sensors were utilized to assess Glu detection in the solution, resulting in an RSD of 3.58%. Thereby indicates the commendable repeatability and reproducibility of NC-ZIFs/CF (Fig. 4c). Furthermore, the peak current of the sensor in response to Glu catalysis maintained approximately 90% of its initial value, even after a month of storage at room temperature in a laboratory environment. This demonstrates its excellent long-term stability (Fig. 4d). These results substantiate that the NC-ZIFs/CF sensor can consistently and reliably detect Glu levels.

Based on the above results, to further explore the practical application of NC-ZIFs/CF, we used the i-t method to measure the concentration of Glu in human serum. The human serum samples were collected from Xiangyang Central Hospital of Hubei University of Arts and Science, and the ethical approval was obtained from the Ethics Service Committees of the hospital (assigned No. 2023-129). We added 100 μL of serum to 10 mL of 0.1 mol/L NaOH solution, and recorded the corresponding current generated by this platform. The corresponding current density recorded was transposed into the Glu concentration utilizing the linear regression equation. The test results are summarized in Table 1. Upon comparison of the test results from normal serum (samples 6–10) with those reported by the biochemical analysis laboratory of a local hospital, it is evident that the RSD was less than 3.56%. Furthermore, the relative error was observed to be less than 0.16 mmol/L. Notably, for sera from hyperglycemic patients (samples 1–5), the sensor obtained a lower RSD (less than 2.67%). This indicates that the NC-ZIFs/CF sensor has better detection performance for hyperglycemia analysis. In summary, compared with similar sensors, NC-ZIFs/CF exhibits excellent performance in aspects such as detection range, detection limit, stability, and detection results of human serum samples. However, its current sensitivity performance is relatively ordinary. These results suggest that the NC-ZIFs/CF sensor

Table 1
Glu detection results of human serum in hospital and in this work.

Sample	Result obtained from the hospital (mmol/L)	Result obtained from this work (mmol/L)	RSD (%)	Bias (mmol/L)
1	17.88	17.51	2.07	−0.37
2	10.72	10.98	2.42	0.26
3	11.25	11.55	2.67	0.3
4	14.82	15.18	2.42	0.36
5	15.83	15.65	2.14	−0.18
6	4.36	4.52	3.34	0.16
7	4.35	4.50	3.56	0.15
8	4.25	4.18	1.65	−0.7
9	4.91	4.80	2.25	−0.11
10	5.14	5.03	2.14	−0.11

is a reliable sensing platform for the detection of Glu in human serum and has promising prospects for application.

In this work, we employed a galvanostatic assembly strategy to rapidly and efficiently cultivate structurally unique nano-caltrop-like ZIFs on the surface of CF in just 40 min, thereby establishing a distinctive electrochemical sensing platform for Glu. The NC-ZIFs/CF serves as a novel electrochemical sensing platform, exhibiting a unique biomimetic enzymatic catalytic activity for Glu, which is characterized by an obvious oxidation current density. Additionally, the sensor has the advantages of a wide measurement range, strong anti-interference ability, low detection limit as well as significant reproducibility, repeatability and stability. Most importantly, the NC-ZIFs/CF sensor demonstrates accurate and reliable detection of blood Glu in the serum of both normal and hyperglycemic patients. Our study highlights the novelty of galvanostatic method assembly as a new strategy for growing nano-ZIFs on conductive substrates, which may provide new ideas for the design of electrocatalytic platforms and other applications in the field of electrochemistry.

Declaration of competing interest

The authors declare that they have no known competing financial interests or personal relationships that could have appeared to influence the work reported in this paper.

Acknowledgments

This work was supported by the National Natural Science Foundation of China (No. 51903062), Special Fund Project for Science and Technology Innovation Strategy of Guangdong Province, China (No. pdjh2022b0426), and the Plan on Enhancing Scientific Research in GMU (No. 02-410-2302330XM).

Supplementary materials

Supplementary material associated with this article can be found, in the online version, at doi:10.1016/j.cclet.2023.109386.

References

[1] H. Furukawa, K.E. Cordova, M. O'Keeffe, O.M. Yaghi, Science 341 (2013) 1230444.
[2] X. Xie, G. Mo, B. Hu, Sens. Actuators B: Chem. 393 (2023) 134263.
[3] L. Liu, Z. Chen, J. Wang, et al., Nat. Chem. 11 (2019) 622–628.
[4] A. Kirchon, L. Feng, H.F. Drake, E.A. Joseph, H.C. Zhou, Chem. Soc. Rev. 47 (2018) 8611–8638.
[5] M. Lv, W. Zhou, H. Tavakoli, et al., Biosens. Bioelectron. 176 (2021) 112947.
[6] T.Y. Chen, Y.J. Huang, C.T. Li, et al., Nano Energy 32 (2017) 19–27.
[7] M. Ding, R.W. Flaig, H.L. Jiang, O.M. Yaghi, Chem. Soc. Rev. 48 (2019) 2783–2828.
[8] L. Yang, S. Zhu, Z. He, et al., Chin. Chem. Lett. 33 (2022) 314–319.
[9] X. Ma, Y. Chai, P. Li, B. Wang, Acc. Chem. Res. 52 (2019) 1461–1470.
[10] W. Wang, H. Liu, Z. Huang, et al., Chin. Chem. Lett. 33 (2022) 4185–4190.
[11] B. Wang, A.P. Cote, H. Furukawa, M. O'Keeffe, O.M. Yaghi, Nature 453 (2008) 207–211.
[12] Y. Liu, H. Cheng, M. Cheng, et al., Chem. Eng. J. 417 (2021) 127914.
[13] P. Kukkar, K.-H. Kim, D. Kukkar, P. Singh, Coord. Chem. Rev. 446 (2021) 214109.
[14] Y. Li, M. Xie, X. Zhang, et al., Sens. Actuators B: Chem. 278 (2019) 126–132.
[15] Z. Wei, W. Zhu, Y. Li, et al., Inorg. Chem. 57 (2018) 8422–8428.
[16] Z. Zhao, Y. Kong, X. Lin, et al., J. Mater. Chem. A 8 (2020) 26119–26129.
[17] C. Guan, X. Liu, W. Ren, et al., Adv. Energy Mater. 7 (2017) 1602391.
[18] T. Liu, P. Li, N. Yao, et al., Adv. Mater. 31 (2019) e1806672.
[19] X. Wei, J. Guo, H. Lian, X. Sun, B. Liu, Sens. Actuators B: Chem. 329 (2021) 129205.
[20] L. Wang, X. Feng, L. Ren, et al., J. Am. Chem. Soc. 137 (2015) 4920–4923.
[21] S. Xu, Y. Zhang, Y. Zhu, et al., Biosens. Bioelectron. 135 (2019) 153–159.
[22] H. Huang, T. Li, M. Jiang, et al., Biosens. Bioelectron. 152 (2020) 112001.
[23] M.V. Chinnamani, A. Hanif, P.K. Kannan, et al., Biosens. Bioelectron. 237 (2023) 115468.
[24] Y. Yan, P. Meng, P. Jinrong, et al., Chin. Chem. Lett. 33 (2022) 4133–4145.
[25] L. Yuan, L. Taotao, Y. Gaojian, et al., Chin. Chem. Lett. 33 (2022) 1913–1916.
[26] W. Li, S. Lv, Y. Wang, L. Zhang, X. Cui, Sens. Actuators B: Chem. 281 (2019) 652–658.
[27] J. Zhou, Y. Li, W. Wang, et al., Biosens. Bioelectron. 164 (2020) 112332.
[28] B. Çakıroğlu, Y.C. Demirci, E. Gökgöz, M. Özacar, Sens. Actuators B: Chem. 282 (2019) 282–289.
[29] J. Ma, J. Li, R. Guo, et al., J. Power Sources 428 (2019) 124–130.
[30] X. Li, T. Liu, Y. Zhang, et al., Adv. Fiber Mater. 4 (2022) 1620–1631.
[31] Q. Hong, Y. Wang, R. Wang, et al., Small 19 (2023) e2206723.
[32] Y. Cai, H. Zhu, W. Zhou, et al., Anal. Chem. 93 (2021) 7275–7282.
[33] K. Kim, J. Kim, Y.S. Bae, ACS Sustain, Chem. Eng. 10 (2022) 11702–11709.
[34] X. Chen, D. Liu, G. Cao, Y. Tang, C. Wu, ACS Appl. Mater. Interfaces 11 (2019) 9374–9384.
[35] Y. Ding, Y. Wang, L. Su, et al., Biosens. Bioelectron. 26 (2010) 542–548.
[36] X. Li, Q. Feng, K. Lu, et al., Biosens. Bioelectron. 171 (2021) 112690.
[37] R.B. Rakhi, P. Nayak, C. Xia, H.N. Alshareef, Sci. Rep. 6 (2016) 36422.
[38] X. Zhang, J. Luo, P. Tang, et al., Sens. Actuators B: Chem. 254 (2018) 272–281.
[39] W. Zhu, J. Wang, W. Zhang, et al., J. Mater. Chem. B 6 (2018) 718–724.
[40] H. Li, C.Y. Guo, C.L. Xu, Biosens. Bioelectron. 63 (2015) 339–346.
[41] K. Dhara, J. Stanley, T. Ramachandran, B.G. Nair, T.G. Satheesh Babu, Sens. Actuators B: Chem. 195 (2014) 197–205.